

## Comparison of single neuron models in terms of synchronization propensity

N. Sungar,<sup>1,2</sup> E. Allaria,<sup>2,3</sup> I. Leyva,<sup>2,4</sup> and F. T. Arecchi<sup>2,5</sup>

<sup>1</sup>California Polytechnic State University, San Luis Obispo, California 93407, USA

<sup>2</sup>Istituto Nazionale di Ottica Applicata, Largo E. Fermi, 6 150125 Florence, Italy

<sup>3</sup>Sincrotrone Trieste, 34012 Basovizza, Trieste, Italy

<sup>4</sup>Universidad Rey Juan Carlos, c/Tulipan s/n, 28933 Mostoles Madrid, Spain

<sup>5</sup>Department of Physics, University of Florence, Florence, Italy

(Received 3 December 2007; accepted 20 June 2008; published online 29 July 2008)

A plausible model for coherent perception is the synchronization of chaotically distributed neural spike trains over wide cortical areas. A recently introduced propensity criterion provides a tool for a quantitative comparison of different neuron models in terms of their ability to synchronize to an applied perturbation. We explore the propensity of several systems and indicate the requirements to be satisfied by a plausible candidate for modeling neuronal activity. Our results show that the conflicting requirements of stability and sensitivity leading to high propensity to synchronization can be satisfied by a strongly nonuniform attractor made of two distinct regions: a saddle focus plus a sufficiently separated saddle node. © 2008 American Institute of Physics.

[DOI: [10.1063/1.2959101](https://doi.org/10.1063/1.2959101)]

In exploring the dynamics of brain systems, it has been established that neuronal information is coded by spikes of electrical activity (each one around 100 millivolts high and lasting 1 millisecond) traveling along the neuron axon. Since spikes are almost identical to each other, relevant information is coded in their time positions, which may be varied by mutual coupling or by other modulation of the control parameters, leading eventually to collective synchronization of large brain areas. A recent review, mainly devoted to central pattern generators (CPG),<sup>1</sup> discusses the clever balance of positive and negative feedback (excitatory and inhibitory couplings, respectively) on each neuron in order to achieve a stable dynamical behavior. This is crucial for all autonomous tasks such as the cardiorespiratory and digestive rhythms, which have to be immune to external perturbations. On the other hand, a cognitive module should be ready to respond to different classes of stimuli and organize the response within a limited time interval. According to the feature binding hypothesis, this is achieved by a temporary spike synchronization of all the neurons of a specific cortical module. We aim to model the relevant dynamical features of this synchronization. For this purpose, a recently introduced criterion of “propensity to synchronization” is discussed for dynamical systems that yield spikes with erratic interspike intervals. The first model system where such a return has been studied in detail was introduced to explain a similar behavior observed in lasers. This is called the heteroclinic chaos model (HC). In this paper, we study Hodgkin–Huxley equations (HH) with the control parameters tuned to values that also lead to this behavior of erratic interspike intervals and the Hindmarsh–Rose (HR) model that was introduced as a simplification of HH and in a suitable parameter range that also provides spikes with erratic repetition. A neurophysiologist would be inclined to

model a neuron in a reductionist way, starting from its component behaviors. We rather take a global approach based on the relevant dynamical features, which are compatible with different classes of model equations. Thus a cognitive neuron is broadly modeled as a chaotic spike generator, whose interspike intervals depend upon an external signal (the bottom-up input stimuli) as well as the setting of some control parameters driven by the top-down perturbations from other brain areas.

### I. INTRODUCTION

Quite a few papers have dealt with the time code in neural processes, some relevant examples being Refs. 1–10. Evidence for time correlations between cortical neurons has been found in laboratory animals where local electrical activity is explored by invasive techniques (microelectrodes sensing the membrane potential of a single axon). In the case of human subjects, noninvasive methods, such as EEG, are used. The evidence for a time code in a neural assembly has been established indirectly, in terms of phase synchronization among filtered EEG signals from separate cortical areas.<sup>8,10</sup>

Looking at brain phenomena from a physicist’s perspective, feature binding is perhaps the most crucial aspect of perception formation.<sup>2,3</sup> The feature binding process is represented by the spread of a synchronized state over a wide cortical area.<sup>3</sup> Considering a specific area or module of the cortex, feature binding consists of the fact that, even though individual neurons of the module receiving different stimuli from other modules are supposed to produce different spike trains, when that module has to respond to a definite feature, its neurons synchronize their trains of spike activity in order to build a coherent collective state. A plausible explanation is that top-down perturbations, provided by the previously

stored information, combine with the bottom-up input to fix the spike timing.<sup>11</sup>

In Sec. II, we analyze the dynamical properties that appear sufficient to establish feature binding. In Sec. III, we introduce the propensity and evaluate it for two dynamical systems that are commonly used to model neurons. Conclusive remarks are given in Sec. IV.

## II. DYNAMICAL PROPERTIES

We visualize a cortical module as made of one or more input neurons receiving an external signal, and transferring the information to the rest of the module by mutual coupling, which we will take as nearest-neighbor coupling. The neurons are modeled as identical dynamical systems. We consider that the module has performed a recognition task when all the neurons behave coherently, i.e., have the same firing patterns. A relevant question is whether feature binding is the result of phase synchronization or spike synchronization. Considering phase synchronization from a dynamical point of view,<sup>12,13</sup> the associated time accuracy is rather poor, since the phase correlation decays smoothly over a wide fraction of the interspike interval (ISI). In fact, if we rescale the ISI to  $2\pi$ , then the phase is defined by the trigonometric function  $\arctan(y/x)$ , with  $y$  and  $x$  being two coupled dynamical variables. Thus the phase changes smoothly over  $\pi$ . Since the membrane potential in the single neuron is a train of spikes, coherent behavior means spike synchronization. Standard spike trains have an average ISI much longer than the spike duration (more than 10 times; in the gamma band oscillations  $\langle \text{ISI} \rangle$  lasts 25 ms whereas the single spike duration is 1 ms). Therefore, synchronization implies accurate spike timing, which is in general more stringent than phase synchronization. In fact, phase synchronization is associated with signals that have a prevailing harmonic component, and hence a power spectrum peaked around a particular frequency, whereas spikes are associated with broad spectra.

A neuron must fulfill two conflicting operational requirements, namely stability and sensitivity. By stability, we mean that neurons should be able to withstand environmental disturbances at room temperature and thus the model should have a highly stable attractor. This conflicts with sensitivity, which implies that a weak input should be effective in stimulating the neuron. Furthermore, the interneuron coupling should be weak enough not to alter the individual dynamics of each neuron. These requirements can be reconciled by a strongly nonuniform attractor made of two distinct regions. These are a saddle focus singularity plus a larger regular region that provides spikes. Indeed, the system is highly stable away from the singularity, and yet very sensitive to an external perturbation around the singularity, since the approach through the stable manifold is associated with a local slowing down and hence has high response to a perturbation.

By adjusting the control parameters, the saddle focus singularity neighborhood can provide either a locally periodic or chaotic tangle as the two behaviors are closely nested in parameter space.<sup>14</sup> We will compare different models in the chaotic regime since, in the periodic regime, the system

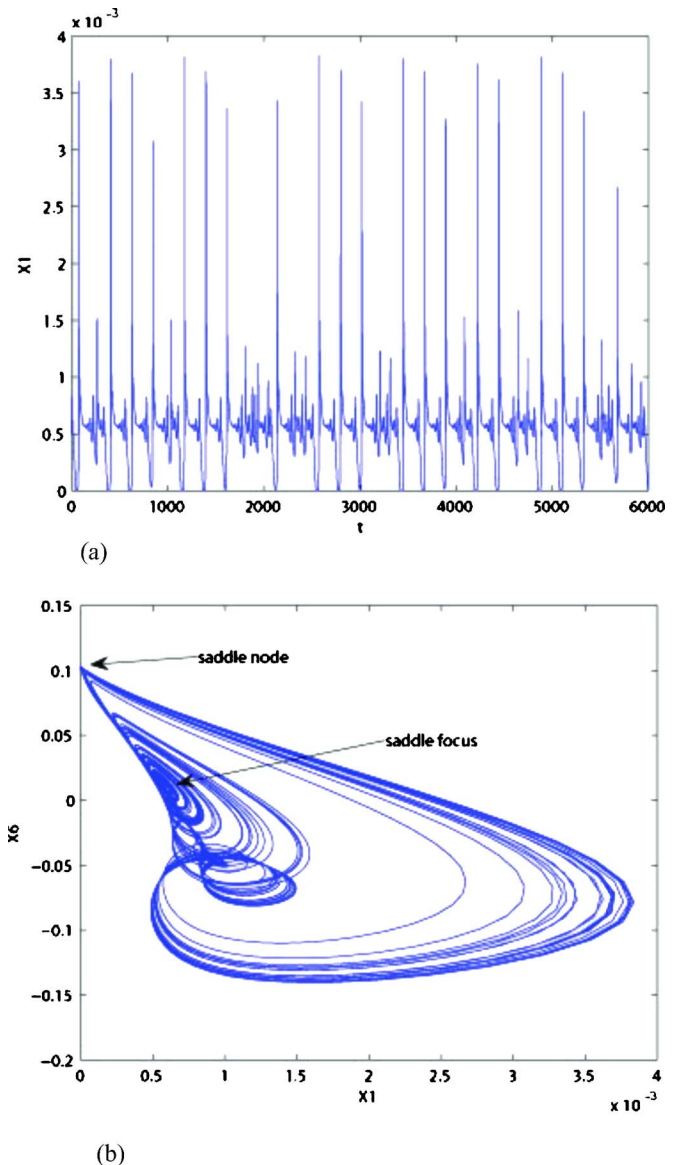


FIG. 1. (Color online) (a) Time series of  $x_1$  for the HC model in the chaotic regime, (b) the phase-space projection over two dynamical variables,  $x_1$  and  $x_6$ .

will adapt to an external stimulus at a cost of time lethargy and energy (high coupling).

We have given substance to these ideas by considering the heteroclinic transfer back and forth between a saddle focus, where the local eigenvalues satisfy the Shilnikov condition for chaos<sup>15</sup> and a saddle node. Such a structure underlies spiking behavior in many neuron models.<sup>16–18</sup> It has also been explored both experimentally<sup>19</sup> and theoretically<sup>14</sup> in the context of a  $\text{CO}_2$  laser with feedback. We will refer to this model as heteroclinic chaos, or HC.<sup>20</sup> The dynamics of this system is characterized by a sequence of spikes with widely fluctuating ISIs and in between the spikes, an irregular signal at a scale much smaller than the spike height as shown in Fig. 1(a). Although in Ref. 20 it was named “homoclinic chaos,” the mere homoclinic return to a saddle focus would not assure a robust regularity (i.e., insensitivity to small disturbances) away from the saddle focus. Instead, the further presence of a saddle node gives the stability away

from the saddle focus, which yields almost identical spikes. The phase-space orbit for HC is a wide regular trajectory with the exception of a small neighborhood of the saddle focus as shown in Fig. 1(b). The exiting trajectories along the unstable manifold reenter the stable one after a large orbit in phase space, corresponding to the heteroclinic approach to a saddle node. The erratic behavior is confined in a small neighborhood of the saddle focus where the Shilnikov condition is fulfilled. Once again, we note that this dynamics is highly nonuniform, in the sense that the sensitivity to small perturbations is large only in the vicinity of the saddle focus. In a mutually coupled assembly of such dynamical systems, only the large spikes become synchronized over the network, whereas the small scales do not contribute to the spread of synchronization.<sup>21</sup>

We thus identify a condition for high propensity to synchronization as the presence within each orbit of two very different amplitude scales. These are a regular region that includes the large spikes and a small chaotic background.<sup>22,23</sup> In the presence of an external driving signal, the spikes can synchronize to this signal.<sup>20</sup> In the case of many coupled systems of this type located on an array, wide parameter ranges can be found within which the individual sites mutually synchronize their spikes.<sup>23</sup>

In order to explore the applicability of this idea to neural models, we study models that can be tuned to have irregular spike intervals. The qualitative descriptions discussed above are satisfied by the Hodgkin–Huxley (HH) model for action potentials<sup>16,24,25</sup> when the parameters are suitably adjusted in order to display a homoclinic return to a saddle singularity.<sup>18</sup> Specifically, in the thermoreceptive version<sup>18,24</sup> of the Hodgkin–Huxley equations, the parameters can be adjusted to meet the Shilnikov condition for chaos. Although thermosensitive neurons are not found to assemble in networks,<sup>2</sup> we study this model since it displays the same features as the HC model, which has already been shown to have high propensity to synchronization.

Another widely used model was introduced by Hindmarsh and Rose (HR).<sup>26</sup> It is characterized by bursts of spikes that occur periodically or chaotically. It has been used to model many neuron processes, both autonomic and cognitive. Even though the phase-space structure of the HR model provides erratic burst intervals, it does not fully satisfy the conditions described above for high propensity since it does not have a saddle focus. However, we study the HR model simply as a comparison to HH. Most of the other single neuron models are lower dimensional, hence they do not exhibit autonomous chaotic behavior. Our study of the nonautonomous Fitz–Hugh–Nagumo model<sup>27</sup> in terms of its propensity to synchronization resulted in very low ( $\sim 0$ ) propensity for all frequency ranges, hence it will not be discussed any further.

It should be noted that when considering HH, we will characterize the time by measuring intervals between individual spikes, while in the HR case, since this model exhibits bursts of spikes, we will measure the interval between bursts. The role of single spikes versus bursts in neural systems is still controversial. Feature binding has been associated with single spike synchronization,<sup>3</sup> while, loosely speaking, the

bursting behavior has recently been associated with central pattern generators (CPG).<sup>28</sup> However, no clear-cut association between cognitive and motor tasks with single spikes and bursts, respectively, has been given so far. A preliminary comparison may be found in Ref. 29 and more recently discussed in Ref. 30. In fact, a different, very clever mathematical approach exists in considering synchronization of bursts<sup>31</sup> while the cognitive role of bursting mechanisms has been explored in Ref. 32.

### III. THE PROPENSITY TO SYNCHRONIZATION

Propensity to synchronization is the key element for feature binding. Given a dynamical system generating a chaotic train of spikes, the relevant question is, how sensitive is the system to perturbations leading to a synchronized state? In the case of a HC system, this question was addressed in Ref. 21.

In order to study the propensity of a system, we perturb one of the parameters of the model by a small-amplitude periodic disturbance. In this approach, the dynamical behavior is modified by tuning some control parameter, having in mind the role of top-down perturbations that change the setting of each neuron besides the bottom-up input stimuli. We study a range of periods around the average ISI (interspike interval) as a way of exploring the sensitivity in a frequency range where any sensible time code should operate. As we explore the sensitivity to a periodic perturbation, we have a kind of Arnold tongue profile with maximum sensitivity around the average ISI.

In order to build an indicator of successful synchronization, we consider the coherence parameter

$$R = \frac{\langle \text{ISI} \rangle}{\delta(\text{ISI})},$$

where  $\delta(\text{ISI})$  is the square root of the ISI variance,  $\delta(\text{ISI}) = (\langle (\text{ISI} - \langle \text{ISI} \rangle)^2 \rangle)^{1/2}$ .  $R$  is of the order of unity for a random distribution of spikes, and very large for an almost periodic sequence.

$R$  is the inverse of the so-called coefficient of variation and provides a sensitive test of synchronization to a periodic perturbation, since it increases dramatically as the system gets more periodic. Starting from the chaotic regime,  $R$  conveniently shows the degree of synchronization for each frequency.

In a chain of coupled systems,  $R$  can differ in general from site to site. However, above a critical coupling parameter for which the chain reaches full spike synchronization, the same  $R$  value holds for all sites<sup>21</sup> and it becomes a collective indicator for the whole chain.

We define the propensity  $P$  as the logarithm (base 10) of the ratio of the  $R$  value under a small periodic perturbation of a control parameter to the  $R$  value for the unperturbed system,

$$P = \log_{10} \frac{R_{\text{pert}}}{R_{\text{free}}}. \quad (1)$$

Of course,  $P$  in general will be a function of the frequency of the periodic perturbation. We would expect that



for a synchronized chain, it is enough to establish  $P$  for a single dynamical system, taken as the input neuron coupled to an external environment; then for some amount of mutual coupling, all the other neurons of the network synchronize to the first one, assuming the same  $P$  value.<sup>21</sup>

In a coupled array, there are thus two aspects to be considered:

- (i) The propensity of a single system (neuron) with respect to an external perturbation.
- (ii) The propagation of the propensity in the chain of coupled systems, starting from an input site where the external perturbation is applied. In the following sections, we will compare the different models from both viewpoints (i) and (ii).

When testing the indicator  $P$  for a single frequency perturbation  $\omega$  for any particular dynamical system,  $P$  will depend on the separation between  $\omega$  and the “natural” frequency  $\omega_o$  associated with the average interspike interval with no perturbation. As for the propagation of  $P(\omega)$  from site to site, we will stress how  $P$  depends on the site position  $x$  for each coupling strength,  $\varepsilon$ . Hence, our aim is to compare  $P(\omega, x)$  for different amounts of input signals and coupling strength.

We compare the propensity for the Hodgkin–Huxley neural model (HH) in the thermoreceptive version<sup>18,24</sup> and the Hindmarsh–Rose (HR)<sup>26</sup> model. In the case of the Hindmarsh–Rose model, we distinguish two different numerical versions, used by different groups, which we denote HR1<sup>33</sup> and HR2.<sup>34</sup>

The results for the two models reported in the following section have been obtained by adding a sinusoidal perturbation to one of the control parameters with an amplitude that is  $\sim 10\%$  of the parameter size. Each system of differential equations has been numerically solved using the fourth-order Runge–Kutta method. A threshold is applied to the output signal to obtain the time intervals between spikes for the HH model and the time interval between bursts for the HR model.

### A. Hodgkin–Huxley model (HH)

For our study, we use the thermosensitive version of the Hodgkin–Huxley model,<sup>18,24,25</sup> which has been proposed to reproduce the spike patterns observed in several experiments on temperature receptor neurons.<sup>35,36</sup> These receptors codify the temperature information into spike trains, and single neurons show a variety of dynamics from excitability to homoclinic chaos, going through periodicity and period doubling chaos, with temperature being the only control parameter. To account for all these behaviors, the classical Hodgkin–Huxley model is modified to include two new slow currents with subthreshold oscillations, independent of the spiking dynamics, as found in the experiments.

The model consists of the following set of equations:

$$\frac{dV}{dt} = - \left( \frac{1}{C} \right) (I_l + I_d + I_r + I_{sd} + I_{sr}), \quad (2)$$

where  $I_l = g_l(V - V_l)$ ,

$$\begin{aligned} I_d &= \rho(T)g_d a_{di}(V - V_d), & I_r &= \rho(T)g_r a_{ri}(V - V_r), \\ I_{sd} &= \rho(T)g_{sd} a_{sd}(V - V_{sd}), & I_{sr} &= \rho(T)g_{sr} a_{sr}(V - V_{sr}), \\ a_{di} &= (1 + e^{-s_d(V - V_{od})})^{-1}, & a_{ri} &= (1 + e^{-s_r(V - V_{or})})^{-1}, \\ a_{sdi} &= (1 + e^{-s_{sd}(V - V_{osd})})^{-1}, \end{aligned} \quad (3)$$

and

$$\begin{aligned} \dot{a}_r &= \frac{\phi(T)(a_{ri} - a_r)}{\tau_r}, & \dot{a}_{sd} &= \frac{\phi(T)(a_{sdi} - a_{sd})}{\tau_{sd}}, \\ \dot{a}_{sr} &= \frac{\phi(T)(-vI_{sd} - \theta a_{sr})}{\tau_{sr}}, \end{aligned} \quad (4)$$

with temperature-dependent variables

$$\phi(T) = A_2^{(T - T_o)/10}, \quad \rho(T) = A_1^{(T - T_o)/10}. \quad (5)$$

Here,  $V$  is the membrane potential of the neuron and  $C$  is the membrane capacitance.  $I_l$  is the leakage current and  $I_d$  and  $I_r$  are currents representing Na and K channels, respectively.  $I_{sd}$  and  $I_{sr}$  are the slow currents that account for the oscillations. More details and the values of the parameters can be found in Ref. 18.

This model yields a period doubling cascade for temperatures greater than  $T = 6.76^\circ\text{C}$ ,<sup>18</sup> followed by homoclinic bifurcation at  $T = 10.66^\circ\text{C}$ , at which point the system satisfies the Shilnikov condition. In our study, we fix the temperature to  $T = 15.5^\circ\text{C}$ , i.e., in the range of homoclinic chaos.

The time series for the membrane potential  $V$  can be seen in Fig. 2(a). The corresponding ISI histogram shows a band centered around  $\omega_o = 0.03$ , as can be observed in Fig. 2(b). The continuous range in the natural frequencies of the system indicates a sensitivity to be driven by an external signal.

First, we study the response of a single neuron when the system is perturbed by adding an external current of the form  $I_e = I_o \sin(\omega t)$ . We considered a perturbation of 10% on the variable  $V$  and therefore set  $I_o = 3.0$  and computed the propensity  $P$  as a function of the external frequency  $\omega$ . The system is found to be very sensitive for a continuous range of external frequencies  $\omega$  above  $\omega_o$ , as can be seen in Fig. 2(c).

Although thermosensitive neurons are not found to assemble in networks,<sup>2</sup> for comparison with HC, we also consider the propagation of propensity  $P$  along a bidirectional, weakly coupled chain of 20 HH neurons. In all the cases, the first element of the chain ( $i = 1$ ) is forced with an external modulation  $I_e = I_o \sin(\omega t)$  where the forcing frequency  $\omega$  is chosen to be 0.1, a frequency for which we have previously obtained a high  $P$  for the single element [Fig. 2(c)]. The rest of the neurons along the array, i.e.,  $i = 2, \dots, 20$ , are not perturbed and  $I$  is set to zero.

In Fig. 3, we show the value of  $P$  along the array for several values of the coupling  $\varepsilon$ . We observe that for weak coupling, the information propagates along the chain as a spike synchronized state. As the coupling becomes stronger, the synchronized state reaches sites farther from the perturbed one, and for  $\varepsilon > 0.07$  the synchronization is spread along the whole chain. Therefore, as in the case of HC, the

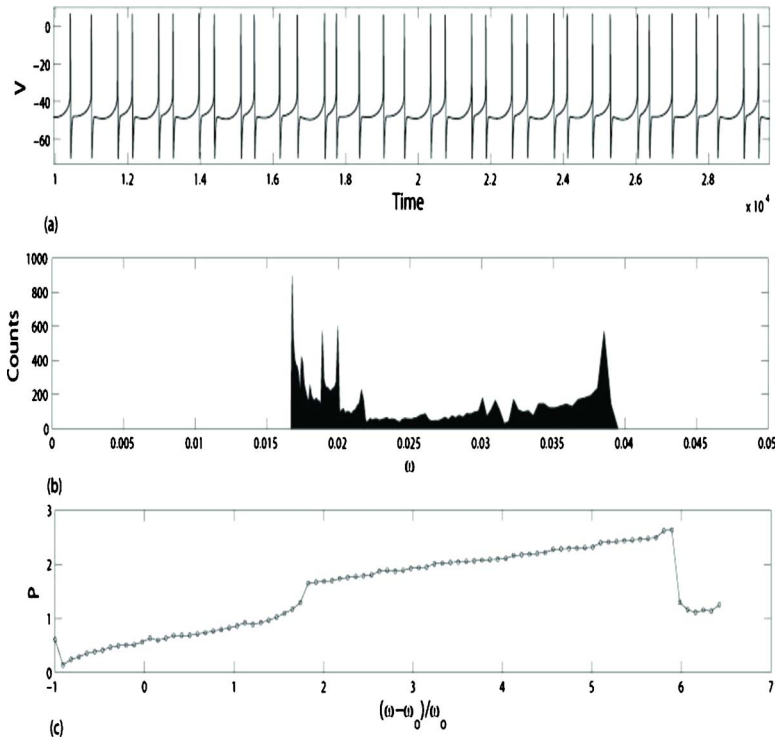


FIG. 2. (Color online) Results for the HH model when  $T=15.5^\circ\text{C}$ . (a) Time series of the membrane potential  $V$ , (b) frequency distribution, (c) propensity vs the normalized distance of the forcing frequency from the natural frequency  $\omega_0$ .

chaotic ISI provides a propensity for synchronization to an external signal and a high enough coupling facilitates the synchronization to be transmitted along a network.

**B. Hindmarsh–Rose model (HR)**

The Hindmarsh–Rose model is described by the following equations:

$$\frac{dx}{dt} = y + 3x^2 - x^3 - z + I, \tag{6}$$

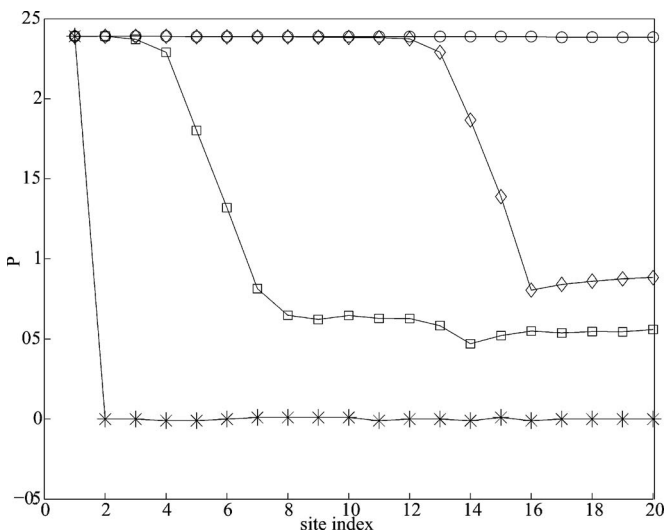


FIG. 3. Propensity for the HH model when  $T=15.5^\circ\text{C}$  vs array site number for a forcing frequency of  $\omega=0.1$ ; for coupling strengths  $\varepsilon=0.01$  (\*),  $0.06$  (□),  $0.065$  (◇), and  $0.07$  (○).

$$\frac{dy}{dt} = 1 - 5x^2 - y, \tag{7}$$

$$\frac{dz}{dt} = s(4(x + 1.6) - z). \tag{8}$$

In HR1, the version in Ref. 33  $s$  is 0.0021, and in HR2, the version in Ref. 34  $s$  is 0.006. For HR1, when  $I=3.281$ , the system has a saddle node at  $(-0.6835, -1.3359, 3.666)$  with eigenvalues  $(-6.7003, 0.1913, 0.0044)$ . For HR2, when  $I=3.0$  the system has a saddle node at  $(-0.7882, -2.1063, -3.2472)$  with eigenvalues  $(-7.7565, 0.1428, 0.0147)$ .

At this input ( $I$ ) value,  $x$  shows bursting behavior with chaotic interburst intervals (IBI). Here the relevant feature is the interburst interval rather than the interspike intervals (ISI) within each burst. The natural frequency,  $\omega_0$ , of the HR1 system is 0.011 and the natural frequency of the HR2 system is 0.0431. A time series for the HR2 system is shown in Fig. 4(a).

We add a sinusoidal perturbation with 10% amplitude to the input parameter  $I$  and compute the propensity  $P$  as a function of the frequency  $\omega$  of the perturbation. The results for HR1 and HR2 are very similar, hence we only show the HR2 results in Figs. 4(b) and 4(c). Figure 4(b) shows the propensity of a single unit as the forcing frequency is varied, and Fig. 4(c) shows the ratio of the system frequency to the forcing frequency  $\omega$ . Perturbation of some of the other parameters produced similar results.

As can be seen in Fig. 4(b), HR2 shows a high propensity for a number of frequencies. However, in contrast to HH, the propensity is high only for a discrete set of frequencies. The system responds with periodic bursting at twice the forc-

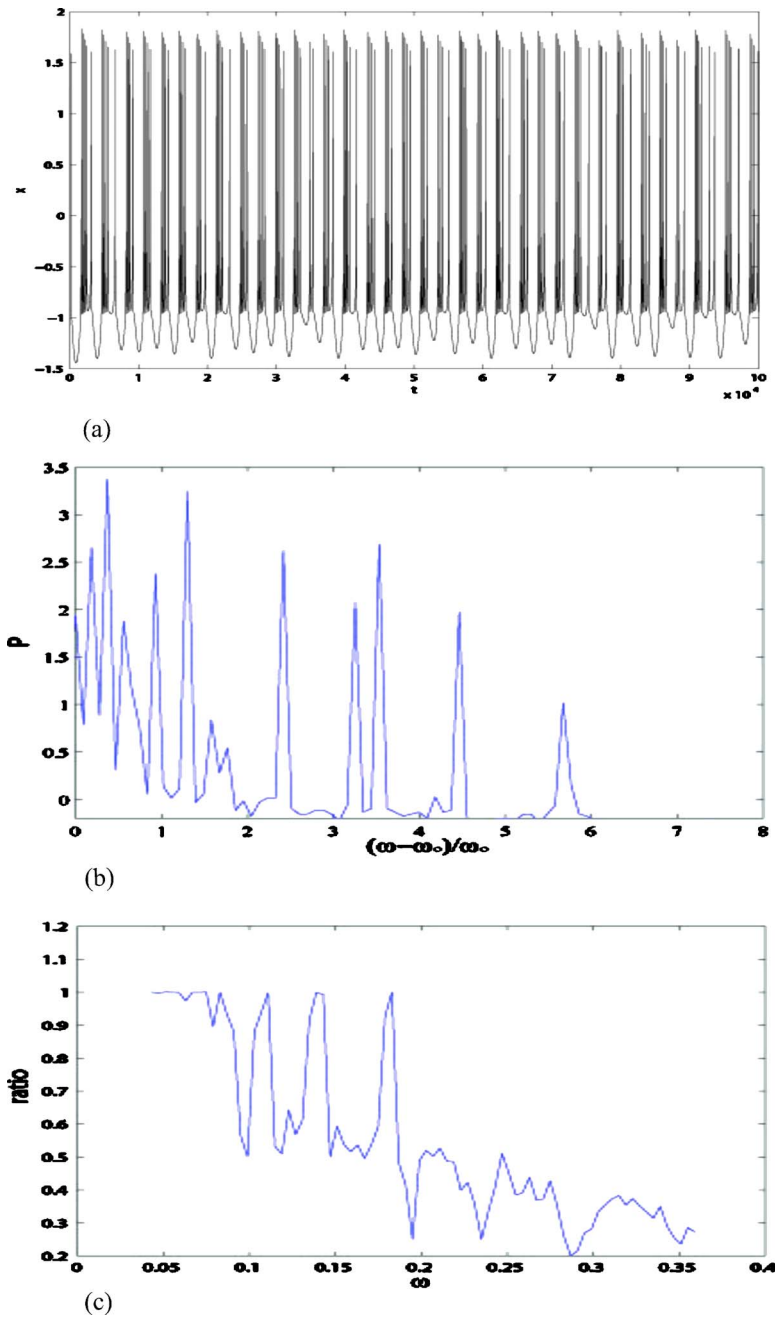


FIG. 4. (Color online) Time series for the HR2 model with  $I=3.0$ , (b) propensity vs the normalized distance of the forcing frequency from the natural frequency  $\omega_0$ , (c) the ratio of the frequency of the system to the forcing frequency  $\omega$ .

ing period when the forcing period is smaller than the refractory period of the bursts. However since this time is much shorter than the average IBI, this effect is seen at frequencies larger than six times the natural frequency for HR1 and three times the natural frequency for HR2 since the IBI for HR2 is roughly one-third of the IBI for HR1.

Next, we couple 19 identical HR2 units with diffusive coupling and perturb the input  $I$  in the first unit along the array with a sinusoidal, 10% amplitude signal. The forcing frequency is set to 0.043, the natural frequency of the model for which high propensity is obtained for a single unit. All the other units along the array are not perturbed. Figure 5 shows the propensity  $P$  as a function of array site number for several coupling strengths. The propagation of burst synchronization is not very effective compared to the spike synchronization seen in HC and HH models. For weak coupling, the

propagation of propensity increases with increasing coupling strength, reaching a maximum in the range  $\varepsilon=0.01-0.025$ . As the coupling strength is increased further, propagation of propensity quickly drops to zero. At these higher coupling strengths, the coupling between unperturbed units overwhelms the influence of the perturbed unit. While the first unit receiving the perturbation shows periodic bursting at the period of the perturbation, the unperturbed units start synchronizing among themselves with chaotic IBI finally reaching full synchronization around a coupling of 0.5.

Using a coupled system of HR neurons, Dhamala *et al.*<sup>37</sup> have presented evidence of two successive transitions to synchronized states, one associated with burst (slow dynamics) and the other with spikes (fast dynamics) as the coupling strength is increased. This is relevant for modeling midbrain dopaminergic neurons, important in reward-mediated learn-

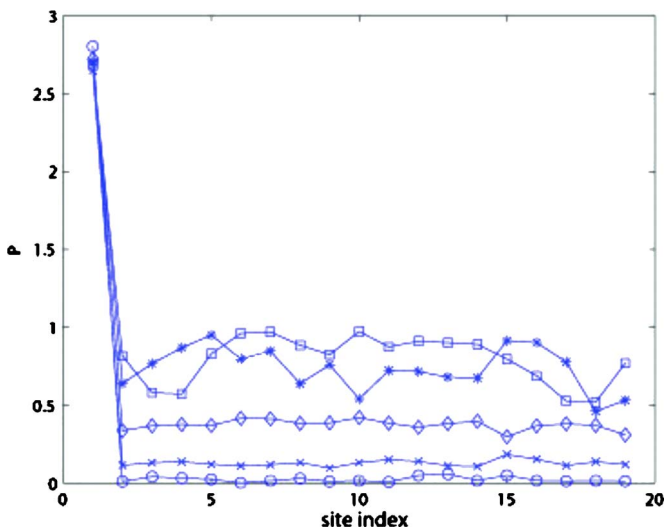


FIG. 5. (Color online) Propensity for the HR2 model vs array site number for a forcing frequency of  $\omega=0.043$ ; for coupling strengths  $\varepsilon=0$  ( $\circ$ ),  $0.01$  ( $*$ ),  $0.02$  ( $\square$ ),  $0.05$  ( $\diamond$ ), and  $0.1$  ( $\times$ ).

ing, which exhibit two modes of action potential firing: spike firing, and burst firing.<sup>38</sup> This behavior does not, however, seem related to the feature binding, which has been associated with spike synchronization.<sup>2,4,39</sup>

#### IV. DISCUSSION AND CONCLUSIONS

The main conclusion of this paper is that a saddle focus can provide variable and easily tunable timing between successive returns. If the return is homoclinic, then the spikes also have a large variability in amplitude. The amplitude can be regularized by adding the heteroclinic connection to a saddle node, provided that the saddle node is sufficiently separated from the saddle focus so that the attractor displays a regular region that is clearly distinct from the chaotic tangle around the saddle focus. These considerations led<sup>21</sup> to a comparison between HC and the Lorenz system, showing how the propensity depends crucially on the topology of the added saddle node. Precisely, the propensity will be high or low depending on whether the added fixed point is located in a regular or chaotic region of the attractor, respectively.

In the periodic regime, it is also possible to obtain results similar to those obtained in the chaotic regime when the two behaviors are closely nested in parameter space, but in this case the propagation of synchronization requires stronger coupling.

Thus, the broadband propensity obtained for the HH model means that any feature with Fourier components within the sensitivity range can be recognized. HR is convenient if the time code is associated with interburst intervals, but its semantic ability is limited only to a restricted number of Fourier components. Furthermore, the timing accuracy in the burst synchronization is reduced with respect to the single spike synchronization in the ratio between the burst duration to the single spike duration. Of course, a burst provides a driving signal more robust than the single spike. Indeed, it is largely used by the neurons of CPG for controlling repetitive actions.<sup>1</sup>

It should also be noted that our study did not involve inclusion of noise or diversity among the elements of the array. In the case of noise, it is reasonable to expect that a reliable perceptual task should be robust to noisy perturbation (the so called “cocktail party effect,” whereby we detect a meaningful conversation hidden in the presence of incoherent disturbances). As for diversity, it has been shown<sup>40,41</sup> to influence the synchronization ability of a coupled array of excitable systems. The property of excitability can emerge as a collective one, by coupling nonexcitable, but HC, individual elements; this matter is dealt with extensively in another paper.<sup>42</sup>

We conclude with some comparisons between chaotic and excitable dynamics as possible models for single neurons. Reference 31 deals with excitable systems ruled by only two coupled (fast and slow) equations. There are two separate attractors, namely a fixed point (rest state) and a limit cycle (repetitive firing), and the transition from one to the other takes place due to the slow variable that moves the fast one from rest to a limit cycle oscillation (burst). Various synchronization regimes are then studied. These are either burst synchronization or spike synchronization (in the latter case, they are spikes within the burst), however no chaotic phenomena occur. Our approach is totally different. Based on the experimental evidence of single spike synchronization,<sup>39</sup> we study dynamical systems yielding single spikes separated by chaotic ISIs and explore synchronization conditions. For communication purposes, encoding associated with single spikes has some virtues that are explored in Ref. 43.

Which one of the two (single spike or burst synchronization) is more plausible for cognitive purposes, or whether the two mechanisms are both present in the brain but apply to different tasks, is a matter that must be decided by neuroscientists. We just state that from the point of view of a time code, single spike synchronization is faster than burst synchronization, and we focused our study mostly on the former case.

<sup>1</sup>M. I. Rabinovich, P. Varona, A. I. Selverston, and H. D. Abarbanel, *Rev. Mod. Phys.* **78**, 1213 (2006).

<sup>2</sup>W. Gerstner and W. M. Kistler, *Spiking Neuron Models (Single Neurons, Populations, Plasticity)* (Cambridge University Press, Cambridge, 2002).

<sup>3</sup>W. Singer and C. M. Gray, *Annu. Rev. Neurosci.* **18**, 555 (1995).

<sup>4</sup>C. von der Malsburg, *The Correlation Theory of Brain Function*, in *Models of Neural Networks II*, edited by E. Domany, K. Schulten, and J. L. van Hemmen (Springer, New York, 1994).

<sup>5</sup>M. Abeles, *Corticonics* (Cambridge University Press, Cambridge, 1991).

<sup>6</sup>M. Abeles, *Firing Rates and Well-timed Events*, in *Models of Neural Networks II*, edited by E. Domany, K. Schulten, and J. L. van Hemmen (Springer, New York, 1994).

<sup>7</sup>R. Ritz and T. J. Sejnowski, *Curr. Opin. Neurobiol.* **7**, 536 (1997).

<sup>8</sup>E. Rodriguez, N. George, J. P. Lachaux, J. Martinerie, B. Renault, and F. Varela, *Nature* **397**, 340 (1999).

<sup>9</sup>K. MacLeod, A. Backer, and G. Laurent, *Nature* **395**, 693 (1998).

<sup>10</sup>J. P. Lachaux, E. Rodriguez, J. Martinerie, and F. J. Varela, *Hum. Brain Mapp.* **8**, 194 (1999).

<sup>11</sup>S. Grossberg, *Am. Sci.* **83**, 438 (1995).

<sup>12</sup>J. Kurths, *Int. J. Bifurcation Chaos Appl. Sci. Eng.* **10** (2000) (special issue).

<sup>13</sup>S. Boccaletti, J. Kurths, G. Osipov, D. L. Valladares, and C. S. Zhou, *Phys. Rep.* **366**, 1 (2002).

<sup>14</sup>A. N. Pisarchik, R. Meucci, and F. T. Arecchi, *Eur. Phys. J. D* **13**, 385 (2001).

<sup>15</sup>L. P. Shilnikov, *Sov. Math. Dokl.* **6**, 163 (1965).

<sup>16</sup>A. L. Hodgkin and A. F. Huxley, *J. Physiol. (London)* **117**, 500 (1952).

- <sup>17</sup>E. M. Izhikevich, *Int. J. Bifurcation Chaos Appl. Sci. Eng.* **10**, 1171 (2000).
- <sup>18</sup>U. Feudel, A. Neiman, X. Pei, W. Wojtenek, H. Braun, M. Huber, and F. Moss, *Chaos* **10**, 231 (2000).
- <sup>19</sup>F. T. Arecchi, R. Meucci, and W. Gadowski, *Phys. Rev. Lett.* **58**, 2205 (1987).
- <sup>20</sup>E. Allaria, F. T. Arecchi, A. Di Garbo, and R. Meucci, *Phys. Rev. Lett.* **86**, 791 (2001).
- <sup>21</sup>F. T. Arecchi, E. Allaria, and I. Leyva, *Phys. Rev. Lett.* **91**, 234101 (2003).
- <sup>22</sup>I. Leyva, E. Allaria, F. T. Arecchi, and S. Boccaletti, *Chaos* **14**, 118 (2004).
- <sup>23</sup>I. Leyva, E. Allaria, S. Boccaletti, and F. T. Arecchi, *Phys. Rev. E* **68**, 066209 (2003).
- <sup>24</sup>C. Zhou and J. Kurths, *Chaos* **13**, 401 (2003).
- <sup>25</sup>H. A. Braun, M. T. Huber, M. Dewald, K. Schafer, and K. Voigt, *Int. J. Bifurcation Chaos Appl. Sci. Eng.* **8**, 881 (1998).
- <sup>26</sup>J. Keener and J. Sneyd, *Mathematical Physiology* (Springer-Verlag, New York, 1998).
- <sup>27</sup>R. FitzHugh, *Biophys. J.* **1**, 445 (1961).
- <sup>28</sup>R. Latorre, F. B. Rodriguez, and P. Varona, *Biol. Cybern.* **95**, 169 (2006).
- <sup>29</sup>Neural Networks **14**(6) (2001) (special issue on Spiking neurons in neuroscience and technology).
- <sup>30</sup>W. Singer, *Scholarpedia* **2**, 1657 (2007).
- <sup>31</sup>E. M. Izhikevich, *SIAM Rev.* **43**, 315 (2001).
- <sup>32</sup>J. Rinzel, *A Formal Classification of Bursting Mechanisms in Excitable Systems*, in *Lecture Notes in Biomath*, Vol. 71 (Springer-Verlag, Berlin, 1987).
- <sup>33</sup>X. J. Wang, *Physica D* **62**, 263 (1993).
- <sup>34</sup>A. Raffone and C. van Leeuwen, *Chaos* **13**, 1090 (2003).
- <sup>35</sup>H. A. Braun, H. Wissing, K. Schafer, and M. C. Hirsch, *Nature* **367**, 270 (1994).
- <sup>36</sup>H. A. Braun, K. Schafer, K. Voigt, R. Peters, F. Bretschneider, X. Pei, L. Wilkens, and F. Moss, *J. Comput. Neurosci.* **4**, 335 (1997).
- <sup>37</sup>M. Dhamala, V. K. Jirsa, and M. Ding, *Phys. Rev. Lett.* **92**, 028101 (2004).
- <sup>38</sup>A. S. Freeman, L. T. Melzer, and B. S. Bunney, *Life Sci.* **36**, 1983 (1985).
- <sup>39</sup>P. Fries, D. Nikolic, and W. Singer, *Trends Neurosci.* **30**, 309 (2007).
- <sup>40</sup>C. S. Zhou, J. Kurths, E. Allaria, S. Boccaletti, R. Meucci, and F. T. Arecchi, *Phys. Rev. E* **67**, 015205 (2003).
- <sup>41</sup>C. J. Tessone, A. Scire, R. Toral, and P. Colet, *Phys. Rev. E* **75**, 016203 (2007).
- <sup>42</sup>M. Ciszak, A. Montina, and F. T. Arecchi, "Spike synchronization of a chaotic array as a phase transition," arXiv:0709.1108v1.
- <sup>43</sup>I. P. Mariño, E. Allaria, R. Meucci, S. Boccaletti, and F. T. Arecchi, *Chaos* **13**, 286 (2003).